



e-ISSN: 2587-246X

ISSN: 2587-2680

Cumhuriyet Sci. J., 41(4) (2020) 908-915

<http://dx.doi.org/10.17776/csj.745443>



Determination of the electrical and thermal properties of Al-Sn-Zn alloys

Canan ALPER BİLLUR^{1,*} , Buket SAATÇI² 

¹Sivas Cumhuriyet University, Sivas Technical Sciences Vocational School, 58140 Sivas/Turkey

²Erciyes University, Department of Physics, 38039 Kayseri/ Turkey

Abstract

In the present work, the electrical resistivity, thermal conductivity and microstructure of the 70 at. % Al-15 at. % Sn-15 at. % Zn alloy have been investigated. The electrical resistivity of the alloy was obtained by four-point probe (DC 4PPT) method. Electrical resistivity measurements are used in conjunction with Wiedeman-Franz (W-F) law and Smith-Palmer (S-P) equations to obtain the thermal conductivity of the alloy. The microstructure parameters of the Al-Sn-Zn ternary alloy were obtained by XRD. The surface and phases of alloy were showed by SEM, and the composition of each phase was determined by EDX.

Article info

History:

Received: 30.05.2020

Accepted: 20.08.2020

Keywords:

Microstructure, Thermo-electrical properties of ternary alloys

1. Introduction

In various engineering applications, one of the areas where Al-Sn based alloys are widely used as a plain bearing especially in internal combustion engines. The microstructure of this alloy consists of phases a-Al and b-Sn. Sn phase provides the low friction coefficient required for bearing applications. New generation motors and hybrid systems bring harder working conditions to plain bearings, so what bearing materials need to have better friction properties [1,2].

In addition, Aluminum alloys have interesting electrochemical behavior and electrical properties [3-11]. Visible changes in the electrochemical behavior of Aluminum have been reported even when there is a small amount of Sn [5-8] or Zn [9-11] are introduced to it as alloying activator elements, these elements shift negative values the pitting potential of Aluminum which allowing the alloy to be used as anode material in batteries or in cathodic protection systems for underwater installations. Because of these advantages, many studies have been conducted

electrochemical behaviour of Al, Al-Sn, Al-Zn and Al-Sn -Zn alloys [12,13].

The main purpose of this study is to examine the thermo-electrical properties of the Al-Sn-Zn alloy and determine how the addition of Sn and Zn elements to the aluminum affects the changes of this property

2. Materials and Method

2.1. Determination of microstructure

The metallic elements were melted depending on the composition of the alloy using 99.99 % pure Al, Sn and Zn in the vacuum furnace. The resulting alloy was poured into the mold with a length of about 2 cm and a diameter of 3 cm [for the details see Refs.14-16].

The obtained samples were cut with a miniton device in a 1 cm radius. Samples were rounded and polished to reveal their microstructure. SEM and EDX measurements were made. From the XRD patterns, the crystal symmetry and cell parameters of the samples were obtained by computer-interfaced advanced diffractometer Bruker AXS D8 XRD [17-22].

*Corresponding author. e-mail addresses : cbillur@cumhuriyet.edu.tr

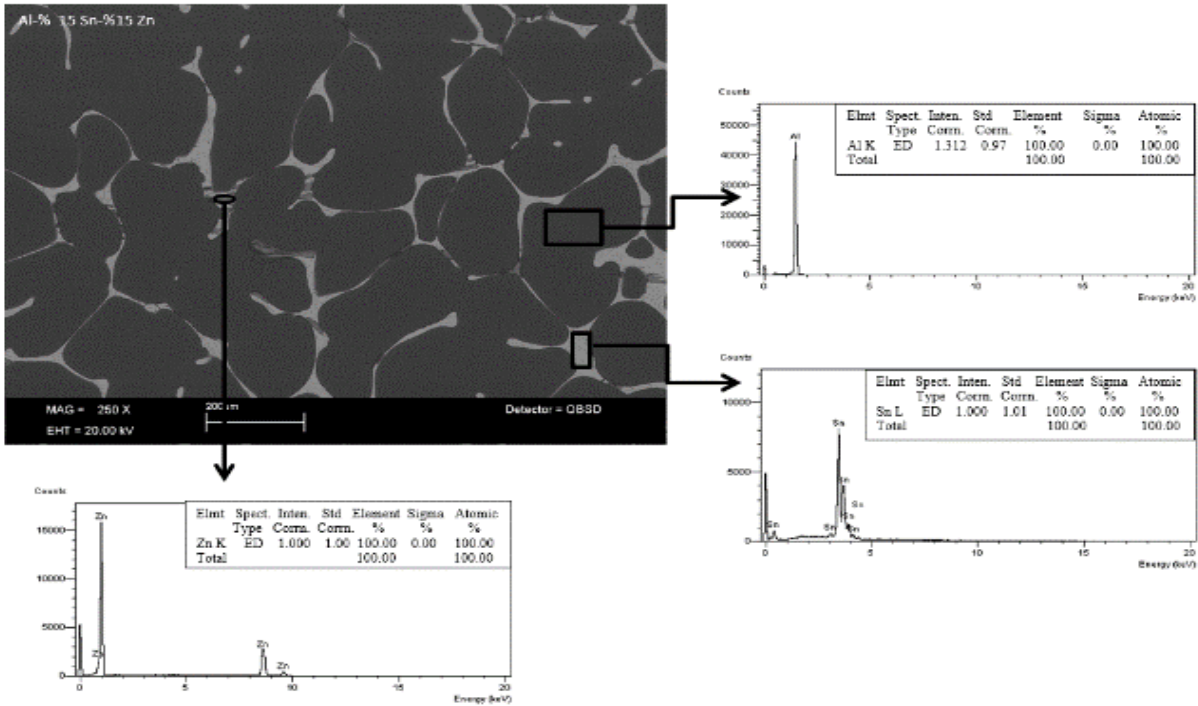


Fig.1. SEM image and EDX analysis of 70 at. % Al-15 at. % Sn-15 at. % Zn ternary alloy.

This machine is measuring between angular ranges $0^\circ < 2\theta < 90^\circ$ with using Bragg-Brentano geometry. The divergence and receiving slit of 1 mm and 0.1 mm is using by the diffractometer. The diffracted rays were counted with a NaI (TI) scintillation detector and the diffraction patterns were scanned in steps of 0.002° (2θ). The XRD patterns of the Al, Sn, and Zn samples were chosen by using the High Score Plus computer program.

2.2 Measurement of electrical properties

By four-point probe (DC 4PPT) method was used to measure the electrical resistivities of the samples. The sample was placed in Nabertherm oven. The oven temperature was adjusted between 300-520 K. The temperature was measured by using standard 0.5 mm K type thermocouples.

Thermocouples were placed very close to the sample to determine the temperature falling on the sample in the most precise way and the temperature of the sample was obtained with a Keithley 2700

multimeter. Standard conversion method was used to achieve current voltage drop [23,24] and the electrical resistance and conductivity measurements were done by this method.

In the DC 4PPT method, measurement errors have been blocked due to probe resistance, spread resistance under each probe, and contact resistances between metal probes and material [15].

However, the temperature coefficient of resistivity (TCR) of the Al-Sn -Zn ternary alloy calculated from the results of electrical resistivity between 300-520 K with the formula below:

$$\alpha_\rho = \left(\frac{1}{\rho_1}\right) \left(\frac{d\rho}{dT}\right) = \left(\frac{1}{\rho_1}\right) \left(\frac{\Delta\rho}{\Delta T}\right) \quad (1)$$

where α_ρ is the TCR in the temperature between $\Delta T = T_2 - T_1$ and $\Delta\rho = \rho_2 - \rho_1$,

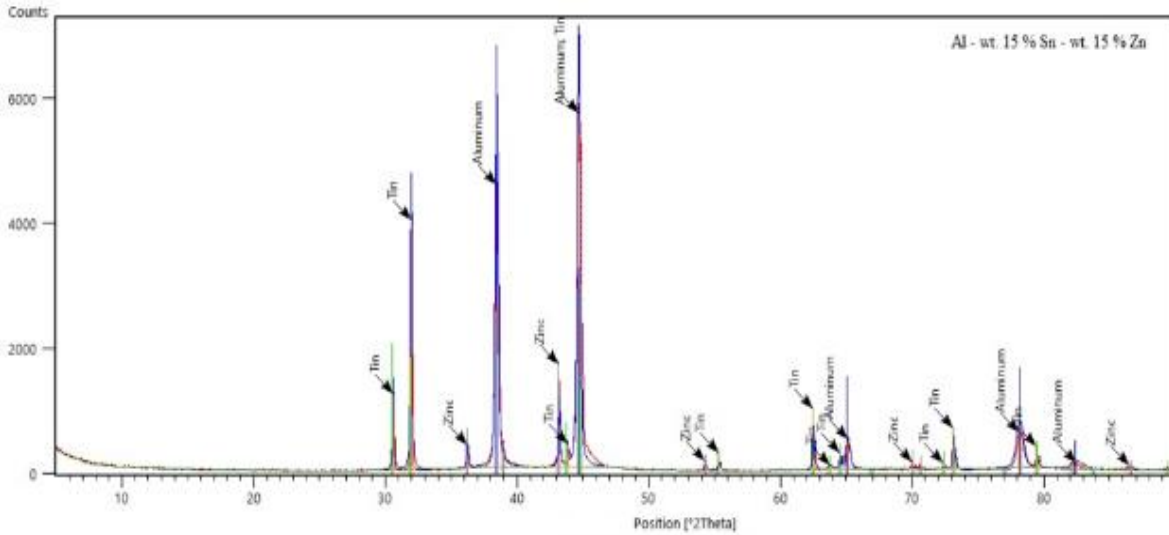


Fig.2. The measured XRD patterns for 70 at. % Al-15 at. % Sn-15 at. % Zn ternary alloys

ρ_1 , is the resistivity at T_1 and ρ_2 , is the resistivity at T_2 .

2.3. Obtaining thermal conductivity

In solids, heat is carried out by various carriers, such as phonons, electrons. There are, however, two types of basic heat carriers in metals: electrons and lattice waves. Accordingly, the components of thermal conductivity are given as follows:

$$\kappa = \kappa_e + \kappa_g \tag{2}$$

where κ_e is the electronic component and κ_g is the lattice component [25].

Table 1. The microstructure properties for 70 at. % Al-15 at. % Sn-15 at. % Zn ternary alloys.

Sample		a(A°)	b(A°)	c(A°)	V(A°) ³	Crystal structure
70 at. % Al-15 at. % Sn-15 at. % Zn	Al	4.0494	4.0494	4.0494	66.40	Cubic
	Sn	5.8200	5.8200	5.8200	107.54	Tetragonal
	Zn	2.6590	2.6590	2.6590	30.23	hexagonal

The relationship between temperature vs. thermal and electrical conductivities can be given by Wiedemann-Franz (W-F) law, which is related to the contribution of free electrons in metals to heat and electricity transport [26]:

$$\frac{\kappa_e}{\sigma T} = L \tag{3}$$

where κ_e , σ , T and L are thermal conductivity, electrical conductivity, temperature, and Lorenz number, respectively. In pure metals, thermal

conductivity is directly proportional to temperature, while electrical conductivity is inversely proportional.

There are experimental studies which have been carried out to measure the thermal conductivity of alloys in the literature. In some of these studies, the thermal conductivity of alloys has been shown to be temperature dependent [27-29].

The W-F law is used to obtain the Lorenz number. In this case, the Lorenz number ($2.45 \times 10^{-8} \text{ W}\Omega/\text{K}^2$) is calculated using the free electron model and the

experimental results of L have temperature dependent even for some pure metals [30]. At the same time, in the literature, it was observed that the L value depends on the properties of the material. The L value was well known for pure materials, but not alloys or composites. We used the electrical conductivity values together with the L coefficient

to find the change in thermal conductivity based on temperature. The Lorenz numbers for tin, aluminium and zinc are $2.30 \times 10^{-8} \text{ W}\Omega/\text{K}^2$, $2.19 \times 10^{-8} \text{ W}\Omega/\text{K}^2$, $2.54 \times 10^{-8} \text{ W}\Omega/\text{K}^2$, respectively. Using these coefficients, the Lorenz number of the alloy is obtained as $2.26 \times 10^{-8} \text{ W}\Omega/\text{K}^2$.

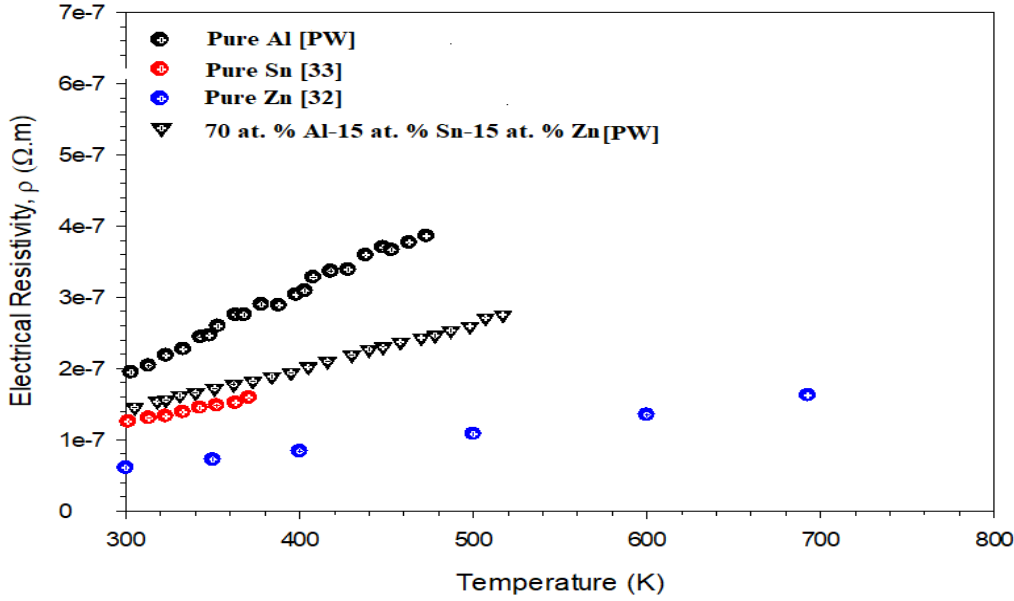


Fig.3. Electrical resistivity of the pure Al, pure Sn, pure Zn and 70 at. % Al-15 at. % Sn-15 at. % Zn alloy system versus temperature.

The W-F law was modified by Smith-Palmer to obtain thermal conductivity of Cu-based alloys from electrical resistivity values. The Smith-Palmer (S-P) formula is given as follows [31]:

$$\kappa = AL\sigma T + B, \tag{4}$$

here the constants B and A are related to the system. The first term on the right side in equation (4) gives the contribution of scattering of electrons by phonons to thermal conductivity.

In addition, the electrical resistivity results for the 300-520 K temperature range are used to calculate

the temperature coefficient of the thermal resistivity (TCTR), α_κ of the Al-Sn-Zn ternary alloy by the following equation,

$$\alpha_\kappa = \left(\frac{1}{\kappa_1}\right) \left(\frac{d\kappa}{dT}\right) = \left(\frac{1}{\kappa_1}\right) \left(\frac{\Delta\kappa}{\Delta T}\right) \tag{5}$$

where α_κ is the TCTR in the temperature between $\Delta T = T_2 - T_1$ and, $\Delta\kappa = \kappa_2 - \kappa_1$, κ_1 is the thermal

resistivity at T_1 and κ_2 is the thermal resistivity at T_2 .

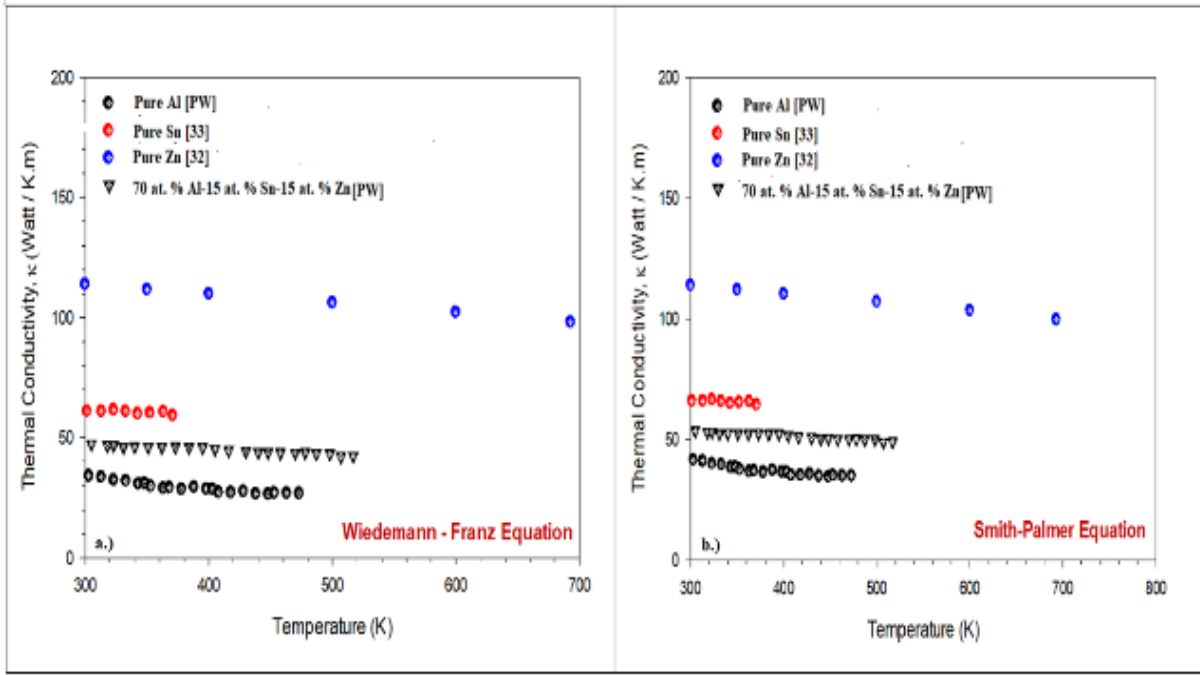


Fig.4. The variations of the thermal conductivity with temperature 70 at. % Al-15 at. % Sn-15 at. % Zn alloy system from a.) the W-F equation b.) the S-P equation

3. Results and Discussion

SEM images and EDX analysis can be seen from Fig 1. Each phase of Al-Sn-Zn alloy was determined by SEM analysis. According to these analyzes, the alloy was homogeneous and no structural defects or impurities were observed. The nominal composition of quantite of the phases was determined by EDX analysis.

XRD, which contains many phase data, gives the most suitable results for the peaks of our alloy. As seen in the Fig.2, The most severe peaks of the Al, Sn and Zn phases were displayed 30° - 50° . Thus, both XRD and EDX analysis show that only three phases are present in the microstructure of the Al-Sn-Zn alloy. The crystal systems and lattice parameters of Al-Sn-Zn alloy were determined by XRD. Details of XRD analysis can be seen from Table 1.

The electrical resistivity values of the alloy and pure elements are shown in Fig.3. It was observed that these values increased with linearly with increasing temperature. Also observed that the electrical resistivity value of the alloy has decreased below the pure Al value with the addition of Sn and Zn. The number of electrons above the Fermi energy in metals provides electrical conduction. Increased temperature in metals increases lattice vibrations i.e

phonons. Thus, the number of collisions made by electrons with each other and phonons increases. As a result, the time between two collisions decreases. This means that electrical resistivity increases. In addition, electrical and thermal conductivities are influenced by many different variables such as sample size and thickness, geometric correction as a function of the distance between the probes, mobility of charge carriers, crystal defects.

Thermal conductivity was calculated using electrical resistivity values. The graphics for both Smith-Palmer and Wiedemann-Franz formulas are given in Fig.4. As shown in Fig.4, the thermal conductivities decrease with increasing temperature. It is observed that the decrease in thermal conductivity is slower compared to the increase of electrical resistivity. The main reason for this decline is rising temperature increases the number of load carriers and lattice vibrations. In metals the increase of lattice vibration is greater than that of load carriers, thermal conductivity decreases. This result was the same for both Smith-Palmer and Wiedemann-Franz. The closeness of the results obtained with these two formulas can be seen in Fig.5

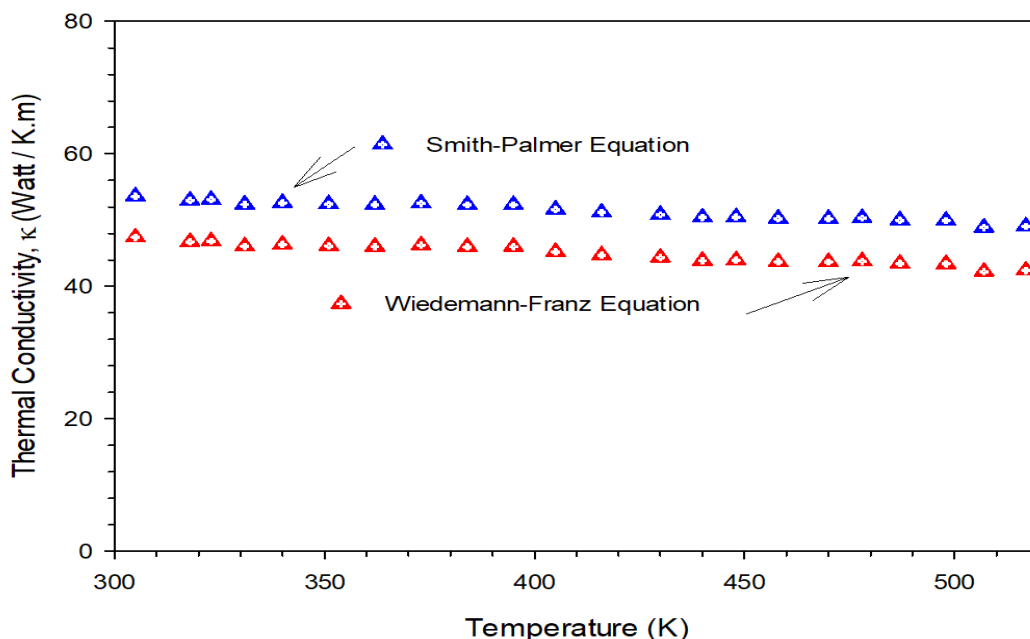


Fig.5. Change of thermal conductivity for 70 at. % Al-15 at. % Sn-15 at. % Zn alloy according to S-P and W-F equations depending on temperature.

4. Conclusion

The structural properties (phases, crystal symmetries, volume...etc) of the samples were determined by the XRD, SEM and EDX measurements.

The electrical resistivity of the alloy was measured by the four point probe (DC 4PPT) in the range of 300-520 K and were seen to increase with increasing temperature as expected. Electrical resistivity of alloy decreased by adding Sn and Zn to pure Al. Based on the electrical measurement results, thermal conductivity values were reached with the help of Wiedeman-Franz and Smith-Palmer laws. The results show that the thermal conductivity values decrease more slowly than the change slope of the electrical resistivity.

Conflicts of interest

Sample sentences if there is no conflict of interest: The authors state that did not have conflict of interests

References

- [1] Lucchetta M.C. Saporiti F. Audebert F., Improvement of surface properties of an Al-Sn-Cu plain bearing alloy produced by rapid solidification. *Journal of Alloys and Compounds*, 805 (2019) 709-717.
- [2] Prucka M., Development of an Engine Stop/Start at Idle System. *SAE*
- [3] *Technical Paper*, 2005-01-0069. Tie D. Guan R. Guo N. Zhao Z. Su N. Li J. and Zhang Y., Effects of Different Heat Treatment on Microstructure, Mechanical and Conductive Properties of Continuous Rheo-Extruded Al-0.9Si-0.6Mg (wt%) Alloy, *Metals*, 5 (2015) 648-655.
- [4] Tie D. Wang Y. Wang X. Guan R. Yan L. Zhang J. Cai Z. Zhao Y. Gao F and Liu H., Microstructure Evolution and Properties Tailoring of Rheo-Extruded Al-Sc-Zr-Fe Conductor via Thermo-Mechanical Treatment, *Metals*, 13 (2020) 845-10.
- [5] Salinas D.R. Bessone J.B., Electrochemical Behavior of Al-5%Zn-0.1%Sn Sacrificial Anode in Aggressive Media: Influence of Its Alloying Elements and the Solidification Structure, *Corrosion*, 47 (1991) 665-673.
- [6] Kliskic M. Radosevic J. Aljinovic L.J., Behaviour of Al-Sn alloy on the negative side of the open-circuit potential, *J. Appl. Electrochem.*, 24 (1994) 814-818.

- [7] Gudic S. Radosevic J. Kliskic M., Impedance and transient study of aluminium barrier-type oxide films, *J. Appl. Electrochem*, 26 (1996) 1027-1035.
- [8] Gudic S. Radosevic J. Kliskic M., Impedance transient study of barrier films on aluminium and Al-Sn alloys. Proceedings of the Symposium on Passivity and its Breakdown. Electrochemical Society, INC, New Jersey, 1997, p. 689.
- [9] Bessone J.B. Flamini D.O. Saidman S.B., Comprehensive model for the activation mechanism of Al-Zn Alloys produced by Indium, *Corros Sci.*, 47 (2005) 95-105.
- [10] Reboul M.C. Gimenez P.H. Rameau J.J., A Proposed Activation Mechanism for Al Anodes, *Corrosion*, 40 (1984) 366-371.
- [11] Tamada A. Tamura Y., The electrochemical characteristics of aluminum galvanic anodes in an arctic seawater, *Corros. Sci.*, 34 (1993) 261-277.
- [12] Khireche S. Boughrara D. Kadri A. Hamadou L. Benbrahim N., Corrosion mechanism of Al, Al-Zn and Al-Zn-Sn alloys in 3wt.%NaCl solution, *Corrosion Science*, 87 (2014) 504-516.
- [13] El Shayeb H.A. Abd El Wahab F.M. Zein El Abedin S., Electrochemical behaviour of Al, Al-Sn, Al-Zn and Al-Zn-Sn alloys in chloride solutions containing stannous ions, *Corrosion Science*, 43 (2001) 655-669.
- [14] Ari M. Saatçi B. Gündüz M. Meydaneri F. Bozoklu M., Microstructure and thermoelectrical transport properties of Cd-Sn alloys, *M. Mater. Charact.*, 59 (2008) 624-630.
- [15] Ari M. Saatçi B. Gündüz M. Payveren M. Durmus S., Thermo-electrical characterization of Sn-Zn alloys, *Mater. Charact.*, 59 (2008) 757-763.
- [16] Saatci B. Ari M. Gündüz M. Meydaneri F. Bozoklu M. Durmus S., Thermal and Electrical Conductivities Of Cd-Zn Alloys, *J. Phys. Condens. Matter*, 18 (2006) 10643-10653.
- [17] Jüskenas R. Mockus Z. Kanapeckaite S. Stalnionis G. Survila A., XRD studies of the phase composition of the electrodeposited copper-rich Cu-Sn alloys, *Electrochimica Acta*, 52 (2006) 928-935.
- [18] Ortiz A.L. Shaw L., X-ray diffraction analysis of a severely plastically deformed aluminum alloy, *Acta Mater.*, 52 (2004) 2185-2197.
- [19] Pinasco M.R. Cordano E. Giovannini M., X-ray diffraction and microstructural study of PFM precious metal dental alloys under different metallurgical conditions, *J. Alloys Compd.*, 289 (1999) 289-298.
- [20] Kasai M. Matsubara E. Saida J. Nakayama M. Uematsu K. Zhang T. Inoue A., Crystallisation behaviour of Cu₆₀Zr₃₀Ti₁₀ bulk glassy alloy, *Mater. Sci. Eng. A*, 375 (2004) 744-748.
- [21] Cullity B.D., Elements of X-Ray Diffraction, third ed., United States of America: Addison-Wesley Publishing Company, Inc, 1967.
- [22] Callister W.D., Materials Science and Engineering-an Introduction, New York: John Wiley and Sons, 1997.
- [23] Zhou D.J., Study on Al-Sn-Si-Cu Bearing Alloy, *J. Light Alloy Fabr. Technol.*, 28 (5) (2000) 44-46.
- [24] G.C., Influence of Silicon Content on Friction and Wear Characteristics of New Al-Sn-Si Alloys, *The Chin. J. Nonferrous Metals*, 8 (9) (1998) 101-105.
- [25] Şahin M. Çadırılı E. Bayram Ü. Ata Esener P., Investigation of the thermoelectrical properties of the Sn_{91.22x}-Zn_{8.8}-Ag_x, *Journal of Thermal Analysis and Calorimetry*, 132 (2018) 317-325.
- [26] Kittel C. Introduction to solid state physics, . 6th ed., New York: Wiley, 1965.
- [27] Li X. Yu J.J., Modeling the effects of Cu variations on the precipitated phases and properties of Al-Zn-Mg-Cu alloys, *J. Mater. Eng. Perform.*, 22 (2013) 2970-2981.
- [28] Hamilton C. Sommers A. Dymek S., A thermal model of friction stir welding applied to Sc-modified Al-Zn-Mg-Cu alloy extrusions, *Int. J. Mach. Tool. Manu.*, 49 (2009) 230-238.
- [29] Murthy K.V.S. Girisha D.P. Keshavamurthy Varol R. T. Koppad P.G., Mechanical and thermal properties of AA7075/TiO₂/Fly ash hybrid composites obtained by hot forging, *Prog. Nat. Sci.-Mater.*, 27 (2017) 474-481.
- [30] Kumar G.S. Prasad G. Pohl R.O., Review experimental determinations of the Lorenz number, *J Mater Sci.*, 28 (1993) 4261-4272.

- [31] Smith C.S., Palmer E.W., Thermal and electric conductivities of copper alloys, *Trans. AIME*, 117 (1935) 225-243.
- [32] Çadırılı E. Kaya H. Büyük U. Şahin M. Üstün E. Gündüz M., Investigation of the thermo-electrical properties of A707 alloys, *Thermochimica Acta*, 673 (2019) 177–184
- [33] Y. Yao, J. Fry, M.E. Fine, L.M. Keer., The Wiedemann–Franz–Lorenz relation for lead-free solder and intermetallic materials, *Acta Mater.*, 61 (2013) 1525–1536.